Transport-Driven Toroidal Rotation in the Tokamak Edge

T. Stoltzfus-Dueck*
Max-Planck-Institut für Plasmaphysik, EURATOM Association, Boltzmannstraße 2, 85748 Garching, Germany
(Received 24 June 2011; published 8 February 2012)

The interaction of passing-ion drift orbits with spatially inhomogeneous but purely diffusive radial transport is demonstrated to cause spontaneous toroidal spin-up in a simple model of the tokamak edge. Physically, major-radial orbit shifts cause orbit-averaged diffusivities to depend on $v_\parallel$, including its sign, leading to residual stress. The resulting pedestal-top intrinsic rotation scales with T_i/B_θ, resembling typical experimental scalings. Additionally, an inboard (outboard) X point enhances co- (counter)current rotation.

DOI: 10.1103/PhysRevLett.108.065002 PACS numbers: 52.25.Fi, 52.25.Xz, 52.55.Fa

Rotation patterns strongly affected by turbulent momentum transport are broadly observed in nature, for example, in atmospheric flows, stellar interiors, and accretion disks [1]. Laboratory tokamak plasmas are observed to rotate toroidally in the absence of applied torque, with edge rotation directed with the plasma current (cocurrent), often proportional to plasma stored energy W over plasma current I_p, and reaching tenths of the ion thermal speed v_{ti} [2,3]. Such intrinsic rotation is of practical as well as fundamental interest, since it stabilizes certain instabilities [4] and contributes to a sheared radial electric field E_r, believed to suppress turbulent transport [5]. Intrinsic rotation is of special importance for the next-generation tokamak ITER, since α heating (nuclear fusion) applies no torque [6].

The intriguing experimental findings have triggered a broad theoretical search for the spontaneous rotation's physical origins. Although neoclassical (collisional transport) effects have been considered [7,8], extensive experimental evidence indicates that turbulence dominates momentum transport [2,9]. Numerical efforts have investigated turbulent momentum transport in the core, both linearly [10,11] and nonlinearly [12]. Models for intrinsic rotation, also primarily core-focused, have treated quasilinear approximations [10,11,13–16], effects of inhomogeneity of the confining magnetic field $\mathbf{B}$ [11,14], nonresonant correlations between the fluctuating radial $\mathbf{E}\times\mathbf{B}$ drift $\tilde{v}_{E,r}$ and parallel velocity $\tilde{v}_\parallel$ [17], and Stringer spin-up type effects [18]. Some scrape-off-layer (SOL) effects have been entertained [19,20] without systematic consideration of the confined plasma's response. Symmetry arguments have strongly constrained gyrokinetic momentum transport in radially local formulations [21].

Momentum transport in the tokamak edge presents particular challenges for theory. The turbulence is strong, with statistics very different from quasilinear estimates [22]. It is also strongly anisotropic, with parallel fluctuation length $L_\parallel$ two orders of magnitude larger than the radial length scale $L_\perp$ characterizing toroidal velocity and equilibrium plasma variation [23–25]. Since parallel fluctuation gradients $k_\parallel \sim 1/L_\parallel$ and the corresponding forces are accordingly weak, turbulently accelerated $\tilde{v}_\parallel$ and the resulting nondiffusive effects [15–17] are smaller than simple diffusive momentum transport by $k_\parallel L_\perp \ll 1$ for realistic edge parameters. Most of these effects are further reduced, actually proportional to a symmetry-breaking $\langle k_\parallel\rangle \ll \langle k_\parallel^2\rangle^{1/2} \sim 1/L_\parallel$ [16,21]. Since $\mathbf{B}$ varies on the scale length of the major radius R_0, the resulting momentum transport effects scale relative to simple diffusion as $L_\perp/R_0 \ll 1$ in the edge [11,14]. Furthermore, the interaction of edge and SOL makes the problem inherently radially nonlocal. For example, the amplitude of the (unnormalized) turbulent fluctuating potential decreases in the radial direction on a short length scale $L_\phi \sim L_\perp$ [26]. Given these experimental facts, the present work analyzes a simplified, purely diffusive kinetic transport model, setting parallel acceleration identically to zero but retaining a model edge and SOL, passing-ion drift orbit excursions, and spatial variation of the diffusivity, finding differential transport of co- and countercurrent ions to cause residual stress and consequent intrinsic rotation levels similar to those seen in experiment.

Analysis begins with a model axisymmetric drift-kinetic transport equation for the ions:

$$\partial_t f_i + v\partial_y f_i - \delta v^2(\sin y)\partial_x f_i - D(y)\partial_x(e^{-x}\partial_x f_i) = 0, \quad (1)$$

representing an ensemble-averaged $L_\perp/a, 1/q, a/R_0, cE_r/B_\theta v_{ti} \ll 1$ reduction of Ref. [27] in a radially thin simple-circular magnetic geometry with reference poloidal, toroidal, and total magnetic field strengths B_θ, B_ϕ, and B_0, respectively, minor radius a, safety factor $q \doteq aB_\phi/R_0B_\theta$, and positive toroidal field [28]. The ion parallel distribution function $f_i(x, y, v, t)$ is normalized to pedestal-top ion density over thermal speed $n_i|_{\text{pt}}/v_{ti}|_{\text{pt}}$, and the parallel velocity v is normalized to $v_{ti}|_{\text{pt}}$, positive for cocurrent motion. The radial position x, poloidal position y, and time t are, respectively, normalized to L_ϕ, a, and the ion transit time $aB_0/B_\theta v_{ti}|_{\text{pt}}$. Transport by turbulent fluctuations is modeled with an inhomogeneous turbulent diffusivity, normalized to $L_\phi^2 B_\theta v_{ti}|_{\rm pt}/aB_0$ and assumed separable, with arbitrary poloidal dependence $D(y)$, decaying exponentially in x. Although phenomenological, the assumed purely diffusive transport provides an important check on the common belief that nondiffusive transport is required for intrinsic rotation. The dimensionless parameter $\delta \doteq q\rho_i|_{\rm pt}/L_\phi$, with ρ_i the thermal ion gyroradius, indicates the passing-ion orbit width relative to the radial turbulence inhomogeneity, taking values around 1/4 for typical ASDEX-Upgrade (AUG) H mode parameters [29]. Collisions are neglected, a reasonable approximation if pedestal-top ions escape without experiencing a collision, roughly for $\nu_{ii}\tau_{\rm cr} < 1$, with ν_{ii} the velocity-dependent ion collision rate and $\tau_{\rm cr}$ the pedestal ion stored energy over the ion heat flux. For thermal pedestal-top ions, $\nu_{ii}\tau_{\rm cr}$ takes values around 1 for typical H modes in AUG, JET, and DIII-D, so superthermal pedestal-top ions tend to exit the plasma collisionlessly while subthermal ones do not. Boundary conditions are $f_i(-\infty, y) \to f_{i0}(v)$, $f_i(\infty, y) \to 0$, $f_i(x<0, y_0) = f_i(x<0, y_0 + 2\pi)$, $f_i(x>0, y_0, v>0) = 0$, and $f_i(x>0, y_0+2\pi, v<0) = 0$, with y_0 the poloidal X-point angle. Equation (1) is invariant to a rigid toroidal rotation $v_{\rm rig}$, normalized to $v_{ti}|_{\rm pt}B_\phi/B_0$ and positive for cocurrent motion, and trivially conserves a simplified toroidal angular momentum $\int(v + v_{\rm rig})f_i\, dv$, particles $\int f_i\, dv$, and energy $\int(1 + v^2/2)f_i\, dv$.

Equation (1) can be approximately analytically solved v by v in steady state for both large and small effective diffusivity $D_{\rm eff}$, results agreeing for $D_{\rm eff} \approx 1$. The solution procedure is briefly described here, with details given in Ref. [28]. Since v appears only as a parameter, v-dependent variable transforms can greatly simplify Eq. (1). First, use new spatial variables

$$\bar{x} \doteq x - \delta v(\cos y - \cos y_0), \tag{2a}$$

$$\bar{y} \doteq D_{y0}^{-1}(v)\int_{y_0}^{y} D(y')e^{-\delta v(\cos y' - \cos y_0)}dy', \tag{2b}$$

with $D_{y0}(v) \doteq \int_{y_0}^{y_0+2\pi} D(y')\exp(-\delta v(\cos y' - \cos y_0))dy'$. Physically, $\bar{x}$ is a drift-surface label and D_{y0} an orbit-averaged diffusivity. Next, for $v<0$, take $\bar{y} \to 1 - \bar{y}$. Finally, transform from $\bar{x}$ to $u \doteq e^{\bar{x}/2}$, obtaining

$$\partial_{\bar{y}} f_i = (D_{\rm eff}/4)(\partial_u^2 f_i - u^{-1}\partial_u f_i) \tag{3}$$

for $f_i(u, \bar{y}, v)$, in which $D_{\rm eff}(v) \doteq D_{y0}(v)/|v|$. Boundary conditions are now $f_i(0, \bar{y}) = f_{i0}(v)$, $f_i(\infty, \bar{y}) \to 0$, $f_i(u<1, 0) = f_i(u<1, 1)$, and $f_i(u>1, 0) = 0$. The normalized flux of particles with velocity v through any closed poloidal contour, $\Gamma(v)$, takes the simple form

$$\Gamma(v) = -\frac{1}{2}D_{y0}(v)u^{-1}\int_0^1 \partial_u f_i\, d\bar{y}, \tag{4}$$

evaluated at any constant $u \le 1$.

Equation (3) shows the original problem to reduce to a one-parameter family of otherwise-identical differential equations. Remarkably, the spatially constant effective diffusivity $D_{\rm eff}$ depends not only on the magnitude of v but also on its sign. Physically, as shown in Fig. 1, this symmetry breaking results from the fact that co- (counter) current ions' drift orbits are displaced major-radially outwards (inwards). For the typical case of turbulent diffusivities larger at the outboard, countercurrent ions experience larger orbit-averaged diffusivities. Preferentially exhausting countercurrent ions represents a cocurrent residual stress, although momentum transport at any given spatial point is purely diffusive.

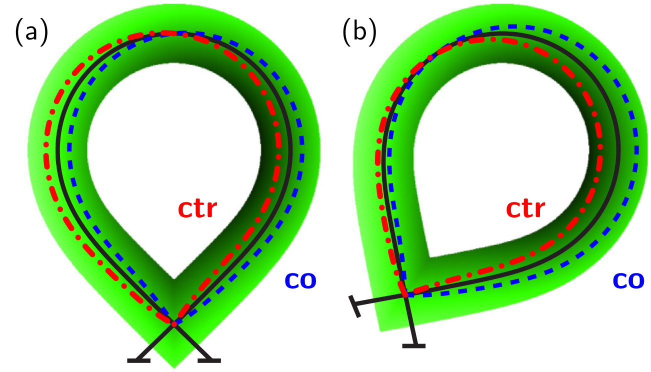

FIG. 1 (color online). Cocurrent (co) and countercurrent (ctr) passing-ion drift orbits over turbulence, plotted for a straight-down (a) and inboard (b) X point. Darker shading indicates stronger diffusivity. Co (ctr) orbits are displaced major-radially outward (inward) as shown, regardless of the sign of B_ϕ or I_p.

In solving Eq. (3), a Laplace transform approach similar to Ref. [30] yielded the exact Green's function

$$G(u, \xi, \tau) = \frac{2u}{D_{\rm eff}\tau}\exp\left(-\frac{\xi^2 + u^2}{D_{\rm eff}\tau}\right)I_1\left(\frac{2u\xi}{D_{\rm eff}\tau}\right), \tag{5}$$

in terms of which the solution may be written as

$$f_i(u, \bar{y}) = f_{i0}e^{-u^2/D_{\rm eff}\bar{y}} + \int_0^1 f_i(\xi, 0)G(u, \xi, \bar{y})\, d\xi. \tag{6}$$

A first-order iterative approximation $f_i^{(1)}$, obtained by setting $f_i(\xi, 0)$ to $f_{i0}\exp(-\xi^2/D_{\rm eff})$ in Eq. (6), was shown to yield an approximate normalized flux $\Gamma/f_{i0}|v|$ with an absolute error strictly less than $\min[0.58D_{\rm eff}^{1/2}(1 - e^{-1/D_{\rm eff}}), 0.75/D_{\rm eff}^{3/2}]$, tight bounds for large $D_{\rm eff}$. For small $D_{\rm eff}$, a two-region solution may be used, representing f_i with a Fourier series for $u < 1$ (edge) and Laplace transforming for $u > 1$ (SOL), requiring continuity in f_i and $\partial_u f_i$ at $u = 1$, except possibly at the single point $u = 1$, $\bar{y} = 0$. The resulting edge and SOL ordinary differential equations possess explicit solutions in terms of modified Bessel functions. Slightly generalizing Ref. [31], one may then show that continuity requires the edge solution to satisfy

$$f_i \approx -\frac{1}{2}D_{\rm eff}^{1/2}\frac{1}{\sqrt{\pi}}\int_0^{\bar{y}}\frac{\partial_u f_i\, dy'}{\sqrt{\bar{y} - y'}} - \frac{1}{8}D_{\rm eff}\int_0^{\bar{y}}\partial_u f_i\, dy' \tag{7}$$

at $u = 1$. The resulting dense matrix for the Fourier coefficients has been solved numerically at various $D_{\rm eff}$, retaining 10 000 modes in $\bar{y}$.

The two approximate solutions

$$\frac{\Gamma}{f_{i0}|v|} \approx \begin{cases} D_{\rm eff}/(1 + a_1 D_{\rm eff}^{1/2} + a_2 D_{\rm eff}), & D_{\rm eff} \lesssim 1 \\ -\frac{1}{2} D_{\rm eff} \int_0^1 \partial_u|_{u=1} (f_i^{(1)}/f_{i0})\, d\bar{y}, & D_{\rm eff} \gtrsim 1 \end{cases} \quad (8)$$

are well-approximated for all $D_{\rm eff}$ by

$$\frac{\Gamma}{f_{i0}|v|} \approx \frac{1}{4} \ln\left(1 + \sum_{j=2}^{8} c_j D_{\rm eff}^{j/2}\right) \approx \ln\left(1 + \frac{D_{\rm eff}}{e^{\gamma}}\right), \quad (9)$$

with $a_1 = 0.8224$, $a_2 = 0.1763$, $c_2 = 4$, $c_3 = -4a_1$, $c_4 = 4a_1 + e^{4/(1+a_1+a_2)} - 5 - 9e^{-4\gamma}$, $c_5 = c_7 = 0$, $c_6 = 8e^{-4\gamma}$, $c_8 = e^{-4\gamma}$, and Euler's constant $\gamma \approx 0.5772$. The second approximation is used for the simplified explicit forms in Eqs. (11) and (12) and corresponding plots, and the first for all other plots. The results of Eqs. (8) and (9) are plotted in Fig. 2(a), along with the large-$D_{\rm eff}$ error bounds.

Explicit forms for the normalized fluxes of particles, momentum, and parallel heat may now be obtained for any specified $f_{i0}(v)$ and $D(y)$. Assuming a Maxwellian $f_{i0}(v) = e^{-v^2/2}/(2\pi)^{1/2}$ and simple ballooning form $D(y) = D_0(1 + d_c \cos y)$, thus

$$D_{\rm eff}(v) = 2\pi D_0 e^{\delta v \cos y_0}[I_0(\delta v) - d_c I_1(\delta v)]/|v|, \quad (10)$$

the relevant flux moments may be reasonably approximated for small δ as

$$\Gamma^p \doteq \int_{-\infty}^{\infty} \Gamma\, dv \approx \sqrt{\frac{2}{\pi}} g_1, \quad (11a)$$

$$\Pi \doteq \int_{-\infty}^{\infty} v\Gamma\, dv \approx 8\delta \sqrt{\frac{2}{\pi}} \left(\cos y_0 - \frac{d_c}{2}\right)(g_3 - g_5), \quad (11b)$$

$$Q_\parallel \doteq \int_{-\infty}^{\infty} \frac{v^2}{2} \Gamma\, dv \approx \sqrt{\frac{2}{\pi}} g_3, \quad (11c)$$

in which $g_p(D_0) \doteq \ln(1 + 2\pi D_0/e^{\gamma} p^{1/2})$. The integrands are plotted in Fig. 2(b), summed over the sign of v. (All plots use representative AUG H mode values $D_0 = 0.033$, $d_c = 0.8$, $y_0 = -5\pi/8$, and $\delta = 0.28$.)

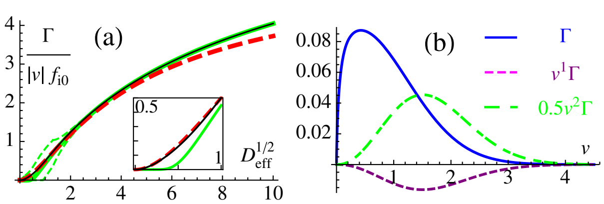

FIG. 2 (color online). (a) Normalized flux as a function of the v-dependent effective diffusivity, with uniform approximation (thin solid black line), small-$D_{\rm eff}$ approximation (thick dashed red line), large-$D_{\rm eff}$ approximation (thick solid green line), and large-$D_{\rm eff}$ error bounds (thin dashed green lines). (b) Speed distribution of fluxes of particles, momentum, and parallel heat, assuming a Maxwellian at the inner boundary.

The total momentum flux, incorporating $v_{\rm rig}$, is just $v_{\rm rig}\Gamma^p + \Pi$. Since toroidal rotation damping is very weak [32], a vanishing momentum input implies that momentum flux must also vanish, resulting in the pedestal-top intrinsic rotation rate

$$v_{\rm int} = -\frac{\Pi}{\Gamma^p} \approx 8\delta(d_c/2 - \cos y_0)\frac{g_3 - g_5}{g_1}, \quad (12)$$

plotted in Fig. 3(a). Alternatively, one may balance an applied neutral-beam injection (NBI) torque with the outward momentum flux resulting from the NBI-driven ion heat flux. For zero pedestal-top toroidal rotation, $v_{\rm rig} = 0$, one must set the unbalanced NBI fraction $f_{\rm unb} \doteq (P_{\rm NBI}^{\rm co} - P_{\rm NBI}^{\rm ctr})/P_{\rm NBI}$ to

$$f_{\rm unb} = \frac{f_c}{2 f_{\rm NBI}} \frac{B_\phi}{B_0} \frac{v_{\rm NBI}}{v_{ti}|_{\rm pt}} \frac{\Pi}{\Gamma^p + Q_\parallel}, \quad (13)$$

in which $f_{\rm NBI}$ is the fraction of heating by NBI, f_c is the fraction of heat transported by ions, and $v_{\rm NBI}$ is the beam ion velocity. The ratio $\Pi/(\Gamma^p + Q_\parallel)$ is plotted in Fig. 3(b). Since $v_{\rm NBI}/v_{ti}|_{\rm pt}$ is typically large, $f_{\rm unb}$ may be a significant fraction of -1, as observed in Ref. [33].

Several features of this solution deserve comment. First, the steady-state results given in Eqs. (12) and (13) are due to a balance between large momentum transport terms [Fig. 2(b)], so they are robust. Relaxation time to the edge intrinsic rotation profile should occur roughly on an ion transport time through the pedestal, $\sim\tau_{\rm cr}$. The v-asymmetric diffusion Π is independent of the toroidal velocity and its radial gradient, so $-\Pi$ represents a residual stress. For typical experimental parameters, it acts in the cocurrent direction with experimentally relevant magnitude. The dimensional intrinsic rotation prediction, given here for small D_0, is

$$v_{\rm int}^{\rm dim} \approx 1.04 \frac{B_\phi}{B_0}\left(\frac{d_c}{2} - \cos y_0\right)\frac{q\rho_i|_{\rm pt}}{L_\phi} v_{ti}|_{\rm pt} \propto \frac{T_i|_{\rm pt}}{B_\theta L_\phi}. \quad (14)$$

The $1/B_\theta$ dependence corresponds to experimentally observed $1/I_p$ scalings [2,3], while proportionality to ion

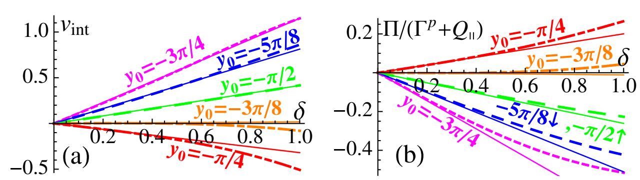

FIG. 3 (color online). Normalized intrinsic rotation velocity $v_{\rm int}$ (a) and unbalanced NBI fraction $\Pi/(\Gamma^p + Q_\parallel)$ (b) plotted as functions of drift orbit width δ for several values of poloidal X-point angle y_0, with numerical integrals (thick dashed lines) and analytical approximations (thin solid lines).

temperature $T_i|_{\rm pt}$ provides an alternative explanation for recent observations [25,34]. Cocurrent spin-up at the L-H transition [2,3] is expected due to the increase in $T_i|_{\rm pt}$ and probable decrease in L_ϕ. The predicted dependence on the X-point poloidal angle has yet to be experimentally tested. The physics presented here may also have implications for internal transport barrier rotation: For outboard-ballooning and radially increasing diffusivity (as outside an internal transport barrier), the asymmetric diffusivity causes a countercurrent core rotation increment, as seen in Ref. [35].

Simplifications used in this model must be kept in mind. The presented calculations omitted both the ∇B drift and the radial electric field E_r, outside the latter's contribution to $v_{\rm rig}$. While the ∇B drift has only a modest qualitative effect, a uniform uncanceled poloidal $\mathbf{E}\times\mathbf{B}$ drift of magnitude approaching $v_{ti}|_{\rm pt}B_\theta/B_0$ may contribute a non-negligible residual stress, a transport effect due to a shifted relation between D_{y0} and $D_{\rm eff}$ [28]. Treatment of sheared E_r effects, $\mathbf{E}\times\mathbf{B}$ divergence, or collisions would require nontrivial extensions to the theory. Direct collisional effects on the rotation-driving flux Π may often be small, since Π results mainly from ions that are somewhat superthermal at the pedestal top [Fig. 2(b)] and, thus, very superthermal at the separatrix, with an accordingly low collision rate. However, lower-energy ions may affect both E_r and the rotation saturation $v_{\rm rig}\Gamma^p$. Finally, recall that the turbulence parameters are taken as an input to the present model, not calculated self-consistently.

In summary, radial displacements of passing-ion orbits and typical tokamak-edge turbulence inhomogeneity are shown to result in orbit-averaged diffusivities that depend on the sign of $v_\parallel$. Even in the absence of nondiffusive effects, this results in residual stress and corresponding pedestal-top intrinsic rotation at experimentally relevant levels. The rotation is cocurrent for typical H mode parameters and scales with $T_i|_{\rm pt}/B_\theta$, in agreement with experimental observations.

Helpful discussions with A. Chankin, G. Hammett, P. Helander, J. Krommes, K. Lackner, O. Maj, R. McDermott, B. Nold, T. Pütterich, C. Rost, P. Schneider, and B. Scott and support from an Alexander von Humboldt Foundation research fellowship are gratefully acknowledged.

*tstoltzf@ipp.mpg.de

[1] L. L. Kichatinov, Geophys. Astrophys. Fluid Dyn. **35**, 93 (1986); U. Frisch, Z. S. She, and P. L. Sulem, Physica (Amsterdam) **28D**, 382 (1987); S. A. Balbus and J. F. Hawley, Rev. Mod. Phys. **70**, 1 (1998); M. S. Miesch and J. Toomre, Annu. Rev. Fluid Mech. **41**, 317 (2009).
[2] J. S. deGrassie, Plasma Phys. Controlled Fusion **51**, 124047 (2009), and references therein.
[3] J. E. Rice *et al.*, Nucl. Fusion **47**, 1618 (2007).
[4] E. Strait *et al.*, Phys. Rev. Lett. **74**, 2483 (1995).
[5] H. Biglari *et al.*, Phys. Fluids B **2**, 1 (1990).
[6] E. J. Doyle *et al.*, Nucl. Fusion **47**, S18 (2007), Sec. 3.5.
[7] C. S. Chang and S. Ku, Phys. Plasmas **15**, 062510 (2008).
[8] A. L. Rogister *et al.*, Nucl. Fusion **42**, 1144 (2002); R. Singh *et al.*, Phys. Plasmas **13**, 042505 (2006); U. Daybelge *et al.*, Nucl. Fusion **49**, 115007 (2009).
[9] S. D. Scott *et al.*, Phys. Rev. Lett. **64**, 531 (1990); W. D. Lee *et al.*, *ibid.* **91**, 205003 (2003); A. Kallenbach *et al.*, Plasma Phys. Controlled Fusion **33**, 595 (1991); J. E. Rice *et al.*, Nucl. Fusion **44**, 379 (2004).
[10] R. R. Dominguez and G. M. Staebler, Phys. Fluids B **5**, 3876 (1993); A. G. Peeters, C. Angioni, and D. Strintzi, Phys. Rev. Lett. **98**, 265003 (2007); A. G. Peeters *et al.*, Phys. Plasmas **16**, 042310 (2009); **16**, 062311 (2009); N. Kluy *et al.*, *ibid.* **16**, 122302 (2009).
[11] Y. Camenen *et al.*, Phys. Rev. Lett. **102**, 125001 (2009); Phys. Plasmas **16**, 062501 (2009).
[12] X. Garbet *et al.*, Phys. Plasmas **9**, 3893 (2002); R. E. Waltz *et al.*, *ibid.* **14**, 122507 (2007); I. Holod and Z. Lin, *ibid.* **15**, 092302 (2008); P. W. Terry *et al.*, *ibid.* **16**, 122305 (2009); W. X. Wang *et al.*, Phys. Rev. Lett. **102**, 035005 (2009); **106**, 085001 (2011).
[13] K. C. Shaing, Phys. Rev. Lett. **86**, 640 (2001); E. S. Yoon and T. S. Hahm, Nucl. Fusion **50**, 064006 (2010); R. Singh *et al.*, Nucl. Fusion **51**, 013002 (2011).
[14] T. S. Hahm *et al.*, Phys. Plasmas **14**, 072302 (2007).
[15] B. Coppi, Nucl. Fusion **42**, 1 (2002); Ö. D. Gürcan *et al.*, Phys. Plasmas **14**, 042306 (2007).
[16] C. J. McDevitt *et al.*, Phys. Rev. Lett. **103**, 205003 (2009); Phys. Plasmas **16**, 052302 (2009); C. J. McDevitt and P. H. Diamond, *ibid.* **16**, 012301 (2009).
[17] P. H. Diamond *et al.*, Phys. Plasmas **15**, 012303 (2008); Nucl. Fusion **49**, 045002 (2009); Ö. D. Gürcan *et al.*, Phys. Plasmas **17**, 112309 (2010).
[18] H. Wobig and J. Kißlinger, Plasma Phys. Controlled Fusion **37**, 893 (1995); A. G. Peeters, Phys. Plasmas **5**, 2399 (1998); V. A. Rozhansky and I. Y. Senichenkov, Plasma Phys. Controlled Fusion **52**, 065003 (2010).
[19] V. Rozhansky and M. Tendler, Phys. Plasmas **1**, 2711 (1994); A. V. Chankin and W. Kerner, Nucl. Fusion **36**, 563 (1996); V. Rozhansky *et al.*, Plasma Phys. Rep. **34**, 730 (2008).
[20] B. LaBombard *et al.*, Nucl. Fusion **44**, 1047 (2004).
[21] A. G. Peeters and C. Angioni, Phys. Plasmas **12**, 072515 (2005); F. I. Parra *et al.*, *ibid.* **18**, 062501 (2011); H. Sugama *et al.*, Plasma Phys. Controlled Fusion **53**, 024004 (2011).
[22] M. Wakatani and A. Hasegawa, Phys. Fluids **27**, 611 (1984); B. D. Scott, Phys. Plasmas **12**, 062314 (2005).
[23] M. Endler, J. Nucl. Mater. **266–269**, 84 (1999); J. Bleuel *et al.*, New J. Phys. **4**, 38 (2002).
[24] T. Pütterich *et al.*, Phys. Rev. Lett. **102**, 025001 (2009).
[25] J. S. deGrassie *et al.*, Nucl. Fusion **49**, 085020 (2009).
[26] C. P. Ritz *et al.*, Phys. Rev. Lett. **65**, 2543 (1990); M. Endler *et al.*, Nucl. Fusion **35**, 1307 (1995); R. A. Moyer *et al.*, J. Nucl. Mater. **241–243**, 633 (1997); **266–269**, 1145 (1999); C. Silva *et al.*, Rev. Sci. Instrum. **75**, 4314 (2004);

B. LaBombard *et al.*, Nucl. Fusion **45**, 1658 (2005); J. Horacek *et al.*, *ibid.* **50**, 105001 (2010).
[27] T. S. Hahm, Phys. Fluids **31**, 2670 (1988).
[28] T. Stoltzfus-Dueck, ''Tokamak-Edge Toroidal Rotation due to Inhomogeneous Transport and Geodesic Curvature'' (to be published).
[29] T. Pütterich, P. Schneider, and E. Wolfrum (private communication).
[30] L. Farnell and W. G. Gibson, J. Comput. Phys. **198**, 65 (2004), Appendix A.1.
[31] K. B. Oldham and J. Spanier, J. Math. Anal. Appl. **39**, 655 (1972).
[32] J. W. Connor *et al.*, Plasma Phys. Controlled Fusion **29**, 919 (1987).
[33] W. M. Solomon *et al.*, Plasma Phys. Controlled Fusion **49**, B313 (2007).
[34] J. E. Rice *et al.*, Phys. Rev. Lett. **106**, 215001 (2011).
[35] J. E. Rice *et al.*, Nucl. Fusion **41**, 277 (2001); Plasma Phys. Controlled Fusion **50**, 124042 (2008).